

Technical Notes

TECHNICAL NOTES are short manuscripts describing new developments or important results of a preliminary nature. These Notes should not exceed 2500 words (where a figure or table counts as 200 words). Following informal review by the Editors, they may be published within a few months of the date of receipt. Style requirements are the same as for regular contributions (see inside back cover).

Low Reynolds Number Effects in a Mach 3 Shock/Turbulent-Boundary-Layer Interaction

M. Ringuette,* M. Wu,† and M. P. Martín‡
Princeton University, Princeton, New Jersey 08544

DOI: 10.2514/1.36213

Nomenclature

C_f	=	skin-friction coefficient
L_{sep}	=	separation length
M	=	freestream Mach number
Re_θ	=	Reynolds number based on θ
T	=	temperature
u	=	velocity in the streamwise direction
v	=	velocity in the spanwise direction
w	=	velocity in the wall-normal direction
δ	=	99% thickness of the incoming boundary layer
δ^*	=	displacement thickness of the incoming boundary layer
δ^+	=	ratio of δ to the wall unit
θ	=	momentum thickness of the incoming boundary layer
ρ	=	density

Subscripts

w	=	value at the wall
∞	=	freestream value

Superscript

'	=	fluctuation from the mean
---	---	---------------------------

I. Introduction

A DIRECT numerical simulation (DNS) of a shock-wave and turbulent boundary-layer interaction for a 24-deg compression ramp configuration at Mach 2.9 and Re_θ of 2300 has been reported by Wu and Martín [1]. The validation of the numerical data was performed against the experimental results of Bookey et al. [2] at the same flow conditions. In that validation, we showed that the upstream boundary layer, the mean wall-pressure distribution, the

size of the separation bubble, and the velocity profile downstream of the interaction are predicted within the experimental uncertainty.

In this Note, we present the validation of the fluctuating wall pressure for the DNS data of Wu and Martín [1] against the recent experiments of Ringuette and Smits [3] at matching conditions. Low Reynolds number effects are demonstrated by comparisons of the size of the separation bubble and the wall-pressure signal with measurements at high Reynolds numbers (on the order of 10^4 – 10^5). The effect of Reynolds number on the turbulence amplification is also studied.

II. Wall-Pressure Signal

For the present analysis, we use the DNS data of Wu and Martín [1]. The incoming boundary-layer conditions for the simulation are as follows: $M = 2.9$, $Re_\theta = 2300$, $\theta = 0.38$ mm, $\delta = 6.4$ mm, $\delta^* = 1.8$ mm, $\delta^+ = 320$, $C_f = 0.00217$, $\rho_\infty = 0.077$ kg/m³, $U_\infty = 609.1$ m/s, and $T_\infty = 107.1$ K.

The mean wall-pressure distribution for the DNS data is given in Fig. 1a, which also shows the experimental data of Bookey et al. [4]; the corner is located at $x = 0$. The nondimensional separation-bubble size L_{sep}/L_c for both the DNS and the experiments is shown in Fig. 1b, which plots the empirical envelope of separation-bubble size versus Reynolds number, determined by Zheltovodov et al. [5]. The characteristic length L_c is defined by Zheltovodov et al. [5] and is not repeated here. For the DNS, the separation and reattachment points are defined as the locations in which the average skin-friction coefficient changes sign, whereas the experimental values of Bookey et al. [4] were obtained using surface oil visualization. The experimental error for this technique can easily be 10%,[§] and is reflected in the error bars on the plot. The separation-bubble size for the DNS and experiments agree within the experimental error and lie within the empirical envelope. The low Reynolds number data reported here confirm the trend of the empirical envelope, indicating a significant increase in separation-bubble size with decreasing Reynolds number. This is due to the increase in viscous effects at the lower Reynolds number, as discussed next.

Figure 2a plots the wall-pressure signal given by the numerical simulation. The results from the reference experiments of Ringuette and Smits [3] are shown in Fig. 2b. The axes of both plots have the same scales. The data are presented at three streamwise locations: inside the separated region at about $x/\delta = -2.2$, at the mean separation point at about $x/\delta = -3$, and in the undisturbed boundary layer upstream of the interaction. We find that the signal behavior of the DNS and experiments is similar, but the simulation has a higher level of fluctuation, which is discussed next. Compared with wall-pressure signal data from high Reynolds number experiments (see Dolling and Murphy [6], for example), the low Reynolds number signals are significantly different. The wall-pressure signals within the separation region and at the separation point do not show the clear intermittency that characterizes high Reynolds number measurements, where the signal jumps from the incoming boundary-layer value to that behind the shock and back again. Instead, the low Reynolds number data indicate a broader range of frequencies with amplitudes between the incoming boundary-layer value and the strongest peak values due to the shock wave. This difference is most likely due to the larger effect of viscosity at the lower Reynolds

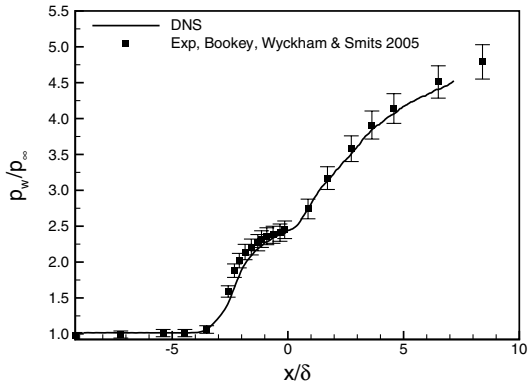
Received 14 December 2007; revision received 26 March 2008; accepted for publication 8 April 2008. Copyright © 2008 by the authors. Published by the American Institute of Aeronautics and Astronautics, Inc., with permission. Copies of this paper may be made for personal or internal use, on condition that the copier pay the \$10.00 per-copy fee to the Copyright Clearance Center, Inc., 222 Rosewood Drive, Danvers, MA 01923; include the code 0001-1452/08 \$10.00 in correspondence with the CCC.

*Postdoctoral Research Associate, Mechanical and Aerospace Engineering Department. Member AIAA.

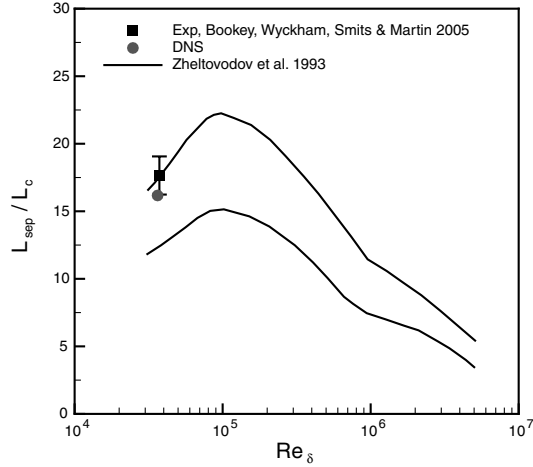
†Ph.D., Mechanical and Aerospace Engineering Department. Student Member AIAA.

‡Assistant Professor, Mechanical and Aerospace Engineering Department. Senior Member AIAA.

[§]Private communication with A. J. Smits, 2006.



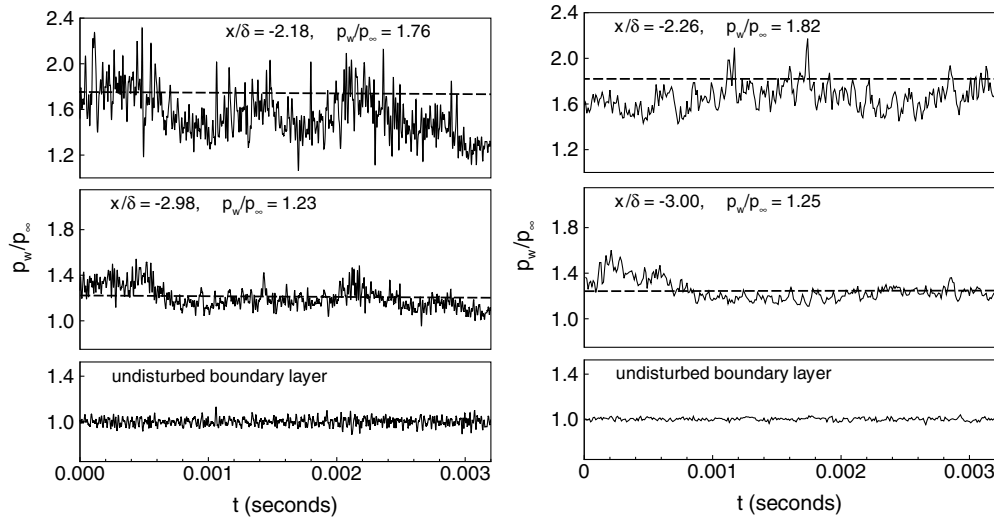
a)



b)

Fig. 1 Plots showing a) mean wall pressure from the DNS compared with the experimental data of Bookey et al. [4] at matching conditions and b) separation-bubble size for the DNS and experiments; error bars are at 10%; both figures are adapted from Wu and Martín [1].

number. The simulations show that the shock does not penetrate as deeply into the boundary layer as in the high Reynolds number case and that it spreads into a compression fan in the lower half of the boundary layer. As a result, the intermittency of the pressure signal is enriched, and the algorithms used to obtain shock intermittency and location from the wall-pressure signal (see Dolling and Brusniak [7], for example) no longer apply.



a)

b)

Fig. 2 Wall-pressure signal from the DNS at three streamwise locations, compared with the experiments of Ringuette and Smits [3]: a) DNS signal, for which the DNS data have been low-pass-filtered at a cutoff frequency of $f\delta_0/U_\infty = 0.55$, equivalent to that of the experiments and b) experimental data at matching conditions; dashed lines indicate mean values.

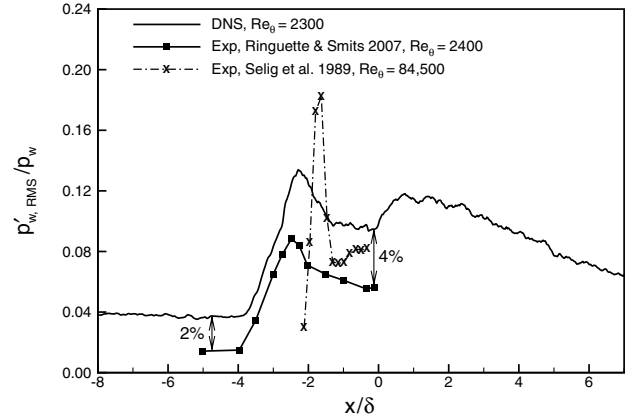


Fig. 3 Distributions of $p'_{w,rms}$ at low and high Reynolds numbers, normalized by the local mean wall pressure p_w .

The rms of the fluctuating wall pressure versus streamwise distance for the simulation and the experiments of Ringuette and Smits [3] is plotted in Fig. 3; the data are normalized by the local mean wall pressure p_w . There is good agreement between the trends of the DNS and the experiments, although the simulation gives somewhat larger values. The synthetically prescribed turbulent structures in the initial condition of the DNS (see Martín [8]) produce slightly higher levels of pressure fluctuations in the incoming boundary layer than are typically found in experiments. These uncorrelated fluctuations can be thought of as noise, such that the fluctuating pressure is the sum of the actual value p'_w and that due to uncorrelated noise p'_n . Then the mean square of the total signal is

$$\overline{(p'_w + p'_n)^2} \approx \overline{(p'_w)^2} + \overline{(p'_n)^2}$$

The quantity $2\overline{p'_w p'_n}$ can be ignored because the correlation is negligible. The noise in the incoming boundary layer can be estimated by assuming that it is equal to the level of pressure fluctuation in the freestream, p'_{∞} , where no pressure fluctuations should be present. The amplification of the noise through the shock wave can then be estimated using the amplification factor of p'_w . The mean square of the freestream pressure fluctuations divided by the square of the local mean wall pressure, $(p'_{\infty})^2/p_w^2$, is about 0.04% upstream of the shock and approximately 0.16% downstream. Taking the square root of these values gives an rms noise level $p'_{n,rms}/p_w$ of 2% in the incoming boundary layer and 4% downstream

of the shock wave and, therefore, an amplification factor for $p'_{n,rms}/p_w$ of 2 through the shock wave. Strictly speaking, the rms of the total wall-pressure signal cannot be decomposed into the sum of the rms of the noise and the actual value. However, Fig. 3 shows that the estimates of 2 and 4% give good approximations of the differences between the DNS and experimental $p'_{w,rms}$ curves upstream and downstream of the shock, respectively.

Also plotted in Fig. 3 are data from the Mach 2.84, $Re_\theta = 84,500$ experiments of Selig et al. [9]. The high Reynolds number peak is substantially larger than the low Reynolds number values and is also narrower. For the low Reynolds number case, the spreading of the shock into a compression fan in the lower part of the boundary layer results in a wider and smaller peak in the $p'_{w,rms}$ curve relative to the high Reynolds number data. Additionally, the location of the low Reynolds number peak is farther upstream, due to the larger separation-bubble size.

Figure 4 gives the premultiplied power spectral density of the wall-pressure signal for the DNS and the experiments of Ringuette and Smits [3] at three different streamwise locations: within the upstream boundary layer, at the mean separation line, and near the peak in the $p'_{w,rms}$ curve. For the experiments, the spectra were computed in MATLAB using Welch's averaged modified periodogram method (`pwelch` command) with a 75,000-point Hamming window, equal to one-twentieth of the total number of experimental data points, and a 50% window overlap. MATLAB was also used to obtain the spectra for the simulations, but the smaller number of samples necessitated the fast Fourier transform to be computed over the entire data set with no windowing. Both spectra have been smoothed over equal logarithmic bins in frequency with 20 bins per decade. Because of a resonance frequency in the pressure transducer used for the experiments, the experimental data are low-pass-filtered with a cutoff frequency of 50 kHz. For reference, the large-eddy frequency U_∞/δ is 90 kHz for the experiments and 95 kHz for the DNS. We find good agreement between the DNS and experimental curves, although the magnitudes of the DNS peaks are somewhat higher. For streamwise locations within the separation region ($x \geq -3\delta$), the data of both studies show broadband low-frequency peaks at similar locations. At $x/\delta = -3.0$, the local maximum for the DNS has a frequency of about 600 Hz and the experimental maximum is located at about 560 Hz, whereas at $x/\delta = -2.2$, the DNS data have a local maximum at about 900 Hz and the experimental peak is at about 580 Hz. The broadband low-frequency peaks correspond to the characteristic frequency of the shock motion.

Both spectra also show broadband peaks at high frequencies (on the order of 10^4 – 10^5 Hz), but there is disagreement between the peak locations of the DNS and the experiments. This is due to the low-pass filtering of the experimental signal, which determines the maximum frequency resolution. The experiments do not resolve the large-eddy frequency, and so the actual peak frequencies should be higher and in better agreement with the DNS. The larger magnitudes of the DNS peaks may be due to the higher values of $p'_{w,rms}$ for the DNS, coupled with limitations of the pressure transducer used for the experiments. The spatial resolution of the pressure transducer has the effect of a low-pass filter with a roll-off frequency of about 16 kHz and therefore reduces the magnitude of the experimental signal above this frequency [3]. Additionally, the low-pass filtering of the transducer output decreases the magnitude of the signal so that it is 3 dB lower at the cutoff frequency [3]. The band of high-frequency peaks is due to the nonuniformity of turbulence structures in the incoming boundary layer [10]. An analysis of the shock motion in the context of the characteristic high and low frequencies observed in the pressure spectra is given in Wu and Martín [10].

Figure 5 plots the mass flux turbulence intensity profiles at multiple streamwise locations for the DNS. Through the interaction, an amplification factor of about 5 is observed. Data from the Mach 2.84 experiments of Selig et al. [9] at $Re_\theta = 84,500$ are also plotted for reference, and it should be noted that the pressure rise through the interaction is the same for the DNS and the experiments. The agreement in the amplification factor for the low and high Reynolds number data indicates that the turbulence amplification is mainly a

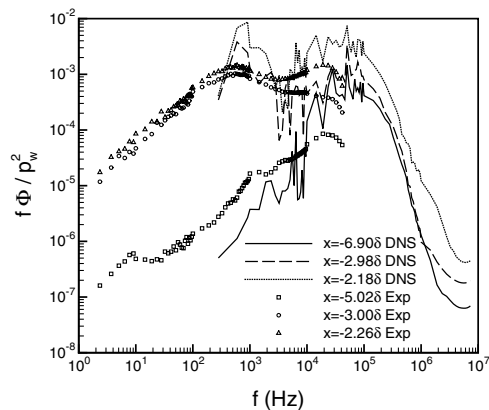


Fig. 4 Premultiplied energy spectral density of the wall-pressure signal at three different streamwise locations for the DNS (lines) and experiments of Ringuette and Smits [3] at matching conditions (symbols); streamwise locations correspond to the incoming boundary layer, the mean separation point, and the peak in the $p'_{w,rms}$ curve, respectively.

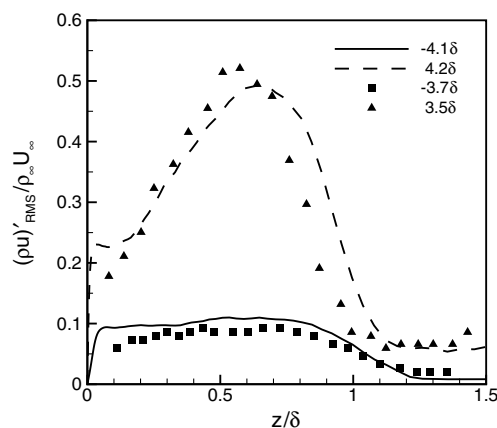


Fig. 5 Mass flux turbulence intensities at different streamwise locations; lines are DNS data and symbols are experimental data from Selig et al. [9] for the same ramp configuration at Mach 2.84 and $Re_\theta = 84,500$.

function of the pressure rise, which is reasonable for a rapid distortion. From the DNS data, the amplification factors for the Reynolds stresses are about 6 for $\overline{\rho u' u'}$ and $\overline{\rho v' v'}$ and approximately 12 for $\overline{\rho w' w'}$. The maximum amplification factor for the Reynolds shear stress, $\overline{\rho u' w'}$, is about 24. The amplification of the Reynolds stresses at low Reynolds number is comparable with that reported in the high Reynolds number, Mach 2.9 experiments of Smits and Muck [11] for a 20-deg ramp angle. The maximum Reynolds shear stress amplification factor for the experiments is about 21; a value lower than that of the DNS is expected, due to the smaller ramp angle.

III. Conclusions

Analysis using the DNS of Wu and Martín [1] and the experiments of Bookey et al. [4] and Ringuette and Smits [3] at matching conditions suggests that low Reynolds number (on the order of 10^3) shock-wave/turbulent-boundary-layer interactions exhibit differences with previous measurements at high Reynolds number (on the order of 10^4 – 10^5). The low Reynolds number effects are due to the greater influence of viscosity and result in a smaller peak in the rms of the wall-pressure fluctuations, an enriched intermittency of the wall-pressure signal, and a substantially larger separation zone. Unlike previous studies at high Reynolds number, the richer wall-pressure signal of the low Reynolds number data cannot be used to determine the location of the shock wave. The primary shock wave does not penetrate as deeply into the boundary layer as for the high Reynolds

number flows, and so it is more accurate to determine the low Reynolds number shock location in the outer region of the boundary layer. However, the low-frequency shock motion (relative to the high frequency that characterizes the undisturbed boundary layer) reported for high Reynolds number flows and the turbulence amplification across the interaction region are not affected by the low Reynolds number condition.

Acknowledgment

This work is supported by the U.S. Air Force Office of Scientific Research under grant AF/9550-06-1-0323.

References

- [1] Wu, M., and Martín, M. P., "Direct Numerical Simulation of Supersonic Turbulent Boundary Layer over a Compression Ramp," *AIAA Journal*, Vol. 45, No. 4, 2007, pp. 879–889. doi:10.2514/1.27021
- [2] Bookey, P., Wyckham, C., Smits, A. J., and Martín, M. P., "New Experimental Data of STBLI at DNS/LES-Accessible Reynolds Numbers," AIAA Paper 2005-309, 2005.
- [3] Ringuette, M. J., and Smits, A. J., "Wall-Pressure Measurements in a Mach 3 Shock-Wave Turbulent Boundary Layer Interaction at a DNS Accessible Reynolds Number," AIAA Paper 2007-4113, 2007.
- [4] Bookey, P., Wyckham, C., and Smits, A., "Experimental Investigations of Mach 3 Shock-Wave Turbulent Boundary Layer Interactions," AIAA Paper 2005-4899, 2005.
- [5] Zheltovodov, A. A., Schülein, E., and Horstman, C., "Development of Separation in the Region Where a Shock Interacts with a Turbulent Boundary Layer Perturbed by Rarefaction Waves," *Journal of Applied Mechanics and Technical Physics*, Vol. 34, No. 3, 1993, pp. 346–354. doi:10.1007/BF00864786
- [6] Dolling, D. S., and Murphy, M. T., "Unsteadiness of the Separation Shock Wave Structure in a Supersonic Compressible Ramp Flowfield," *AIAA Journal*, Vol. 21, No. 6, 1983, pp. 1628–1634.
- [7] Dolling, D. S., and Brusniak, L., "Separation Shock Motion in Fin, Cylinder, and Compression Ramp-Induced Turbulent Interactions," *AIAA Journal*, Vol. 27, No. 6, 1989, pp. 734–742.
- [8] Martín, M. P., "Direct Numerical Simulation of Hypersonic Turbulent Boundary Layers, Part 1: Initialization and Comparison with Experiments," *Journal of Fluid Mechanics*, Vol. 570, Jan. 2007, pp. 347–364. doi:10.1017/S0022112006003107
- [9] Selig, M. S., Muck, K.-C., Dussauge, J. P., and Smits, A. J., "Turbulence Structure in a Shock Wave/Turbulent Boundary-Layer Interaction," *AIAA Journal*, Vol. 27, No. 7, 1989, pp. 862–869.
- [10] Wu, M., and Martín, M. P., "Analysis of Shock Motion in Shockwave and Turbulent Boundary Layer Interaction Using DNS Data," *Journal of Fluid Mechanics*, Vol. 594, Jan. 2008, pp. 71–83.
- [11] Smits, A. J., and Muck, K.-C., "Experimental Study of Three Shock Wave/Turbulent Boundary Layer Interactions," *Journal of Fluid Mechanics*, Vol. 182, Sept. 1987, pp. 291–314. doi:10.1017/S0022112087002349

D. Gaitonde
Associate Editor